eJSE International

*Special Issue: Electronic Journal of Structural Engineering 13(1) 2013*

# VERTICAL DYNAMIC INTERACTION OF TRAINS AND RAIL STEEL BRIDGES

Yan Q SUN[1,3*], Colin COLE[1,3], Maksym SPIRYAGIN[1,3] and Manicka DHANASEKAR[2,3]

[1]*Centre for Railway Engineering, CQ University, Rockhampton, QLD 4702, Australia*

[2]*Queensland University of Technology, Brisbane, Australia*

[3]*CRC for Rail Innovation, Brisbane, Australia*

*Email:* y.q.sun@cqu.edu.au

ABSTRACT: Rail steel bridges are vulnerable to high impact forces due to the passage of trains; unfortunately the determination of these transient impact forces is not straightforward as these are affected by a large number of parameters, including the wagon design, the wheel-rail contact and the design parameters of the bridge deck and track, as well as the operational parameters – wheel load and speed. To determine these impact forces, a detailed rail train-track/bridge dynamic interaction model has been developed, which includes a comprehensive train model using multi-body dynamics approach and a flexible track/bridge model using Euler–Bernoulli beam theory. Single and multi-span bridges have been modelled to examine their dynamic characteristics. From the single span bridge, the train critical speed is determined; the minimum distance of two peak loadings is found to affect the train critical speed. The impact factor and the dynamic characteristics are discussed.

*Keywords: train-track/bridge interaction, train critical speed, impact factor, and dynamic factor*

## 1 INTRODUCTION

Usage of ageing bridges is a challenging and complex engineering problem as these bridges are generally embedded with damage. With the ongoing increase in train axle loads (for example, 20T in the early seventies to 30T in recent times) and speed (passenger trains travel at 160km/h), there is a pressing need to examine the ability of existing rail bridges to carry increasing loads at higher train speeds. Up to now most of rail bridges have been designed only according to static analysis. Actually, the maximum deflection of a rail bridge and the maximum impact force on a rail bridge significantly depend on the dynamic interaction between wheel and rail and the dynamic characteristics of train and bridge. For high speed or heavy trains a dynamic analysis is necessary because of the potential for resonance of the bridge structures. However, the evaluation of the dynamic responses of rail bridges subjected to high-speed train moving loadings is complicated in nature because the dynamic behaviours of bridges are influenced by the interactions between train and bridge structures, and between the components of the trains as well.

The modelling and study of train-bridge interaction dynamics are an important issue not only for the design of the bridge but also for monitoring and maintenance of bridges. Simulations can contribute to the better understanding of live load components in a bridge design code. Meanwhile, the assessments of train and bridge stability and their components fatigue, life cycle analysis, investigations of structural damage and degradation that contribute to maintenance issues can be conducted based on the simulation results. Therefore, a lot of new modelling and studies on train-bridge interaction dynamics have appeared in the recent literature. Based on the recent published papers, the modelling of train-bridge interaction dynamics can be divided into the following four categories:

- Moving masses on bridge structures presented by using beam theory or moving masses on finite element bridge models [6], [8], [9], [12] and [16],
- Multi-body dynamic (MBD) train models on beam bridges presented by using beam theory [2],
- Multi-body dynamic (MBD) train models on finite element bridge models [3], [4], [5], [10], [11], [13], [14] and [15].
- Finite element train models on finite element bridge models [1] and [7].

These models have been applied for many investigations and analyses. The purposes and aims of these studies can be also divided into the following four categories:

- New Modelling Methods: Establishment of modelling methods for the train-bridge interaction dynamics, using modal superposition [2], [7]; the Pseudo Excitation Method (PEM) by transforming the non-stationary random excitations of track irregularities into deterministic time-history excitations [10]; and new methods using finite element methods [13]
- Modelling of Transitions: Transitions are the change of track stiffness from the ballasted conventional track to the bridge-deck based slab or ballasted track. Bridge dynamic behaviours, including: rail vehicle and bridge dynamic responses (displacement and forces) due to track and bridge transitions (usually the bridge has higher stiffness) [2]; rail vehicle and bridge dynamic responses are modelled similar to track geometry irregularities [3], [5], [7], [11]. It is reported [3] that the vehicle accelerations and wheel relative displacements increase significantly when the train is on the onset of crossing the bridge. Two common indices (L/V ratio and lateral track force) [5] are used to assess the potential for derailment of those trains passing over the bridge at different speeds. The simulation results [11] confirm that the elastic slab mats between slab track and bridge can reduce vibration transmitted from rails into the bridge; bridge dynamic response due to random excitation [1]; bridge dynamic (or impact) response due to train moving [6], [8], [14] and [15]. It is indicated [6] that adding of a ballast bed can decrease the natural frequencies of the bridge and hence can decrease the maximum displacement values, but it strongly depends on the velocity as well as the stiffness of the ballast bed itself.
- Spans of Bridges: The effect of the number of spans of the continuous beam on the impact response of the continuous beams is studied [8], and it is shown that the more the number of spans, the smaller the impact response is for the displacement. It is indicated [14] that the dynamic responses of the bridge is significantly amplified in the vicinity of the critical speed, which is decided by the fundamental natural frequency of bridge and the effective beating interval produced by the train; rail vehicle and bridge dynamic responses due to earthquakes [4], which are considered as the input of typical seismic waves with different propagation velocities to the train–bridge system. The critical train speeds are determined based on running safety criteria during earthquakes of various intensities.
- Rail vehicle and bridge dynamic characterisation: Based on the simulation results, it is indicated [5] that the resonance of a bridge can occur in both the lateral and torsional vibrations, as well as in the vertical vibration. From the study in [9], it is shown that the two-span continuous beam has two critical velocities causing two resonance responses, which depends on the first and second natural frequency of the beam and the moving velocity.
- Rail bridge fatigue damage: The critical locations in a bridge span are identified with the simulated results of the global FE stress analysis [12]. Local stress analysis is carried out to obtain the hot-spot stresses, which are used to evaluate fatigue damage and predict the remaining life of the bridge. Principal stress histories of bridge components [16] are obtained by using a refined FE model of the bridge under the passage of a freight train, and are then combined with the plain material S–N curve in order to identify the most fatigue-critical locations.

In order to investigate the bridge dynamic behaviours and characteristics due to train moving loading, and to determine the impact factor on a bridge more accurately and correctly, a rail train-track/bridge dynamic interaction model, including a detailed rail train model using the multi-body dynamics approach and a flexible track/bridge modelling using Euler–Bernoulli beam theory, was generated using Gensys software in this paper. Two kinds of bridges were selected for the simulations. For the first kind of bridge, the bridge resonance characteristic is examined, and the train critical speed is determined. One of the important parameters – the minimum distance between two peak loadings, which influence the train critical speed, is identified through the simulations. The impact factor based on the vertical deflection and the dynamic factor based on the dynamic wheel load are present and discussed.

## 2 FUNDAMENTAL OF BEAM BRIDGE DYNAMICS DUE TO MOVING RAIL VEHICLES

### *2.1 Multi-span Continuous Euler–Bernoulli Beam Modelling*

As stated in the Introduction, the most of rail bridges can be modelled as beams using the beam theory. Euler–Bernoulli beam theory is a simple one, which can provide a means of calculating the load-carrying and vertical deflection characteristics of longitudinal beams subjecting to vertical loads only. Another theory is called the Timoshenko beam theory that can account for shear deformation and is applicable for thick beams. A continuous multi-span Euler–Bernoulli beam is illustrated to deduce its dynamic equation, as shown in Fig. 1, with elastically restrained at the supports $Q_j(t)$ (j = 1, 2, …, $N_s$ ($N_s$ – support number)) and subjected to a system of moving loads $P_i(t)$ (i = 1, 2, …, $N_w$ ($N_w$ – wheelset number)).

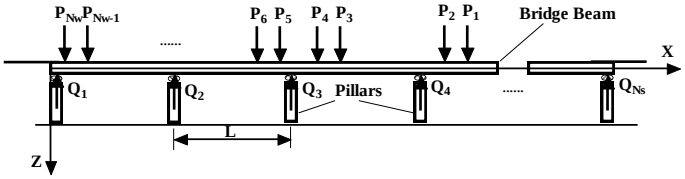


Figure 1 Bridge Beam

The dynamic bridge beam equation can be obtained by Euler-Lagrange equation. The Lagrangian can be written as:

$$L = \frac{1}{2}\rho A\left(\frac{\partial w}{\partial t}\right)^2 - \frac{1}{2}EI\left(\frac{\partial^2 w}{\partial x^2}\right)^2 + q(x,t)w(x,t) \quad (1)$$

Where $\rho$ is the mass density, $A$ is the cross-section area, $w(x,t)$ is the vertical deflection of the beam in the Z direction at the position $x$, $E$ is the elastic modulus and $I$ is the second moment of area of the beam's cross-section, $q(x)$ is the external load. In Eq. (1), the first term represents the kinetic energy, the second one the potential energy due to internal forces, and the last one the potential energy due to the external load $q(x)$, which is written based on Fig. 1 as:

$$q(x,t) = -\sum_{i=1}^{N_s} Q_i\delta(x-x_i) + \sum_{j=1}^{N_w} P_j\delta(x-x_j)\cdot\left[H(t-t_j) - H(t-t_j-\Delta t_j)\right] \quad (2)$$

Where $N_s$ is the pillar support number, $Q_i$ is the $i^{th}$ pillar's reaction force, $\delta(\cdot)$ is the Dirac delta function, $N_w$ is the wheelset number passing the bridge, $P_i$ is the wheel-rail contact force under the $j^{th}$ wheelset, $H(\cdot)$ is the unit step function, $t_i$ is the arriving time of the $j^{th}$ wheelset at the beam, $\Delta t_i$ is the time of the $j^{th}$ wheelset passing over the beam.

According to the Euler-Lagrange equation:

$$\frac{\partial L}{\partial w} - \frac{\partial}{\partial t}\left(\frac{\partial L}{\partial \dot{w}}\right) + \frac{\partial^2}{\partial x^2}\left(\frac{\partial L}{\partial w_{xx}}\right) = 0$$

for a dynamic Euler-Bernoulli beam, the Euler-Lagrange equation is:

$$\rho A\frac{\partial^2 w}{\partial t^2} + \frac{\partial^2}{\partial x^2}\left(EI\frac{\partial^2 w}{\partial x^2}\right) = q(x,t) \quad (3)$$

If the beam internal damping is taken into consideration, Eq. (3) is changed into:

$$\rho A\frac{\partial^2 w}{\partial t^2} + C\frac{\partial w}{\partial t} + EI\frac{\partial^4 w}{\partial x^4} = q(x,t) \quad (4)$$

Where $C$ is the viscous damping coefficient. The vertical deflection $w(x,t)$ can be obtained using modal superposition as given in Eq. (5),

$$w(x,t) = \sum_{h=1}^{\infty} N_z(h,x)\cdot W_h(t) \quad (5)$$

where $N_z(h, x)$ is the $h^{th}$ mode shape function of vertical deflection $w(x,t)$, $W_h(t)$ is the $h^{th}$ mode time coefficient of vertical deflection $w(x,t)$. By substituting Eq. (5) into Eq. (4), we modify the partial differential Eq. (4) into ordinary differential equations shown in Eq. (6) below:

$$\ddot{W}_h + 2\xi_h\omega_h\cdot\dot{W}_h + \omega_h^2 W_h = \frac{q}{m_h}, \quad (h = 1,2,\ldots,\infty) \quad (6)$$

Where $\omega_h$, $\xi_h$, and $m_h$ are the modal frequency, the damping ratio and the modal mass of the $h^{th}$ mode respectively, which can be expressed by complex trigonometric functions for the bridge beam with more than 2 spans. However, for a single span,

$$\omega_h = \left(\frac{h\pi}{L}\right)^2\sqrt{\frac{EI}{\rho A}}, \quad \xi_h = \frac{C}{2\rho A\omega_h} \text{ and } m_h = \rho A.$$

The solution of Eq. (6) can be obtained by a mathematical expression or through any numerical integration method, and then through Eq. (5), the deflection at any point on the beam can be obtained.

### *2.2 Finite Beam Element Modelling*

The multi-span continuous bridge beam, as shown in Fig. 1, can be divided into smaller beam elements. Such a beam element is shown in Fig. 2.

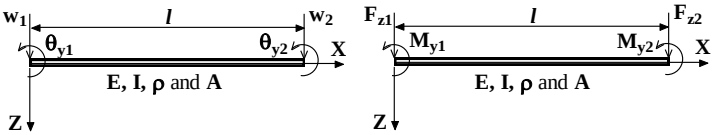


Figure 2 Single Beam Element

Based on Fig. 2, the mass matrix and stiffness matrix of element can be:

$$m_e = \frac{\rho Al}{420}\begin{bmatrix} 156 & 22l & 54 & -13l \\ 22l & 4l^2 & 13l & -3l^2 \\ 54 & 13l & 156 & -22l \\ -13l & -3l^2 & -22l & 4l^2 \end{bmatrix}, \quad k_e = \frac{EI}{l^3}\begin{bmatrix} 12 & 6l & -12 & 6l \\ 6l & 4l^2 & -6l & 2l^2 \\ -12 & -6l & 12 & -6l \\ 6l & 2l^2 & -6l & 4l^2 \end{bmatrix}$$

From these smaller elements, the whole mass matrix and stiffness matrix of bridge beam can be assembled, and the governing equation of bridge beam dynamics can be written as:

$$\mathbf{M}\ddot{\mathbf{D}} + \mathbf{C}\dot{\mathbf{D}} + \mathbf{K}\mathbf{D} = \mathbf{R} \qquad (7)$$

where **M**, **C** and **K** are the mass, damping and stiffness matrixes, $\mathbf{D} = \{w_1\ \theta_{y1}\ w_2\ \theta_{y2}\ \dots\ w_n\ \theta_{yn}\}^T$ is the nodal displacement vector (n is the node number), and $\mathbf{R} = \{F_{z1}\ M_{y1}\ F_{z2}\ M_{y2}\ \dots\ F_{zn}\ M_{yn}\}^T$ is the nodal force vector . In Eq. (7), the Rayleigh damping can be considered as: $\mathbf{C} = \alpha\mathbf{M} + \beta\mathbf{K}$ ($\alpha$ and $\beta$ are the constants). Eq. (7) can be solved by using the modal uncoupled method or through any numerical integration method.

## 3 TRAIN-TRACK-BRIDGE MODELLING

### *3.1 Train Modelling*

A typical passenger train, as shown in Fig. 3 (a), is selected for modelling using Gensys software package. This train consists of two cars and each car weight is 57 tonnes.

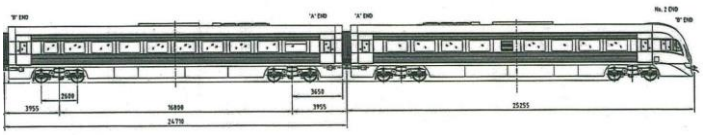

(a) Passenger Train

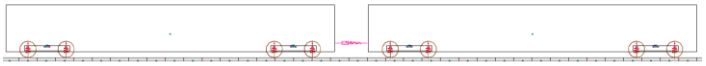

(b) Train Modelling in Gensys

Figure 3 Train and Train Modelling

Based on the limited dimension data (shown in Fig. 3 (a)), the train model is generated using Gensys and is shown in Fig. 3 (b). In a vehicle modelling, one car body and two bogie frames are considered as the rigid bodies with six degrees of freedom (DOFs) each, while four wheelsets are also considered as the rigid bodies with five DOFs each because its pitch rotation DOF is fixed. A stiffness element is required to connect the car body to the ground in longitudinal direction. The descriptions of the connections between the car body and bogie frames are as follows [17], [18]:

- At the centre of the centre bearing rim, two stiffness elements are used to connect the car body and the bogie frame in the lateral and longitudinal directions.
- On the left and right frames of a bogie, four stiffness elements and four damping elements are used to connect the car body and bogie frames in the vertical direction, two friction blocks with flexibility in the longitudinal direction.
- Each of two steering arms in each bogie is modelled as a damping element in the direction specified by the coupling's attachment points.

The descriptions of the connections between the bogie frame and wheelset are as follows:

- Two coil springs in vertical direction and six damping elements in the longitudinal, lateral and vertical directions are used to connect the bogie frame and a wheelset.
- Three friction blocks with flexibility are used to model the axle box friction in the longitudinal, lateral and vertical directions.

The basic parameters relating to the train modelling is given in Appendix - I.

### *3.2 Track & Bridge Modelling*

In this paper, the rail bridge structure is only considered as a beam structure. The beam theory or finite beam element method discussed in the Section 2 is used for rail bridge modelling. The use of a beam in Gensys is the combination of Euler–Bernoulli beam theory and finite beam element method. The beam is defined as an Euler–Bernoulli beam connected to many masses. Fig. 4 (a) shows the track and two-span rail bridge modelling. It allows the suspended masses (wheels) to vertically connect to the beam through a stiffness value (e.g., 200 MN/m), which can be the combination of rail pad, fastener and ballast stiffness, as shown in Fig. 4 (b). On other hand, it also allows the masses (beam segments) to be longitudinally rigid attached to the beam through bending stiffness EI. Therefore, the track and the bridge modelling using Gensys include the three beam modelling aspects – the rail Euler–Bernoulli beam comprising of several beam segments vertically supported by the stiffness and damping elements representing the combinations of stiffness and damping of rail pad, ballast and subgrade, the rail bridge Euler–Bernoulli beam comprising of several beam segments vertically supported by piers, and the other rail Euler–Bernoulli beam. The pier is modelled as the stiffness (e.g., 80e6 N/m) and damping element,

which only vertically connects the bridge beam with the ground.

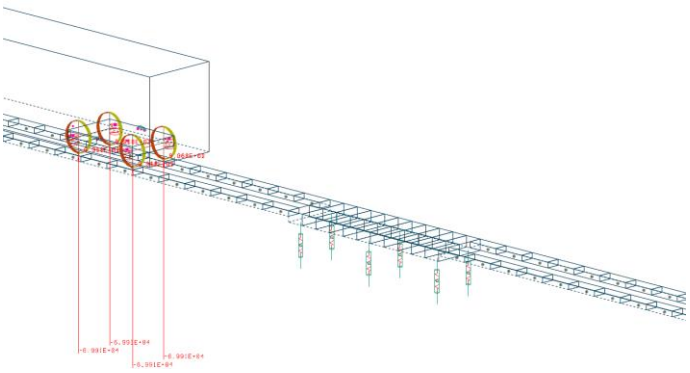

(a) Track-bridge modelling

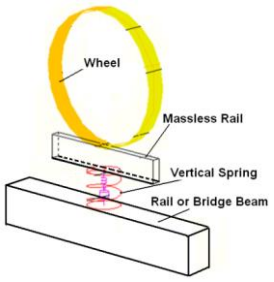


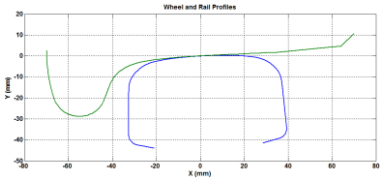


(b) Rail connection to bridge (c) Wheel-rail Profiles

Figure 4 Track-Bridge Modelling

In Fig. 4 (a), a total of 96 beam segments each 1.25m long are used for the track modelling and 11 segments each 0.657m long for the bridge modelling. The wheel and rail profiles shown in Fig. 4 (c) are chosen for the modelling of the contact characteristics. Instead of the consideration of one or two wheel-rail contact points, three different wheel-rail contact points can be in contact simultaneously and are considered in the wheel-rail modelling. Through three spring elements normal to three wheel-rail contact points, the normal wheel-rail contact forces are determined. The calculations of tangent creep forces at three wheel-rail contact surfaces are made in a lookup table calculated using Kalkar creep theory.

## 4 SIMULATIONS

In this section, two types of simulations are conducted. One is for the single span bridge in order to investigate the rail bridge's resonance characteristics due to moving train, and the other is the two-span bridge in order to compare the strain values measured on the bridge with the simulated results. In both simulations, an integration method in Gensys, similar to the two step Runge-Kutta method with step size control which can make backsteps if the tolerance is not met, is selected. The time step is set at 0.0001s.

### *4.1 Single Span Bridge*

The track and bridge modelling is the same as that shown in Fig. 4 except that there is no pier in the middle span of the bridge deck. In order to determine the critical train speed, at which the bridge has the maximum deflection within 0 ~ 400 km/h, the following parameters are assumed and listed in Table 1 for the bridge.

Table 1 Basic Parameters

| Young's Modulus E (GPa) | Second Moment of Area I ($m^4$) | Single Span Length L (m) | Weight (kg/m) |
|---|---|---|---|
| 200 | $7.25\times10^{-4}$ | 6.57 | 1726.8 |

Based on the above parameters, the fundamental natural frequency of the bridge is:

$$f_{n0} = \frac{1}{2\pi}\left(\frac{\pi}{L}\right)^2\sqrt{\frac{EI}{m}} = 10.545\ (\text{Hz}) \qquad (8)$$

Based on Eq. (8), the critical train speed is:

$$V_{cr} = d \times f_{n0} \times 3.6 \quad (\text{km/h}) \qquad (9)$$

Where $d$ is defined as the minimum distance of two effective loadings.

Figs. 5 and 6 show the time histories of the vertical deflections of each bridge beam segment and the wheel load of each wheelset at the train speeds of 80, 200, 310 and 380 km/h.

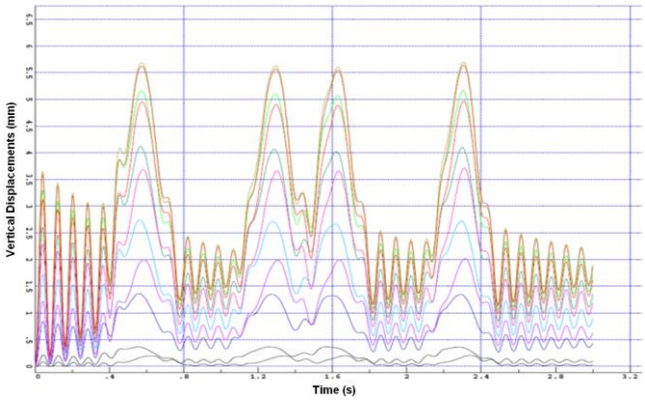


(a) At Speed of 80 km/h

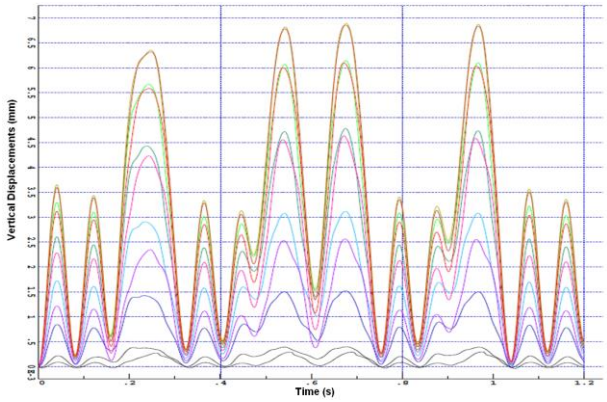


(b) At Speed of 200 km/h

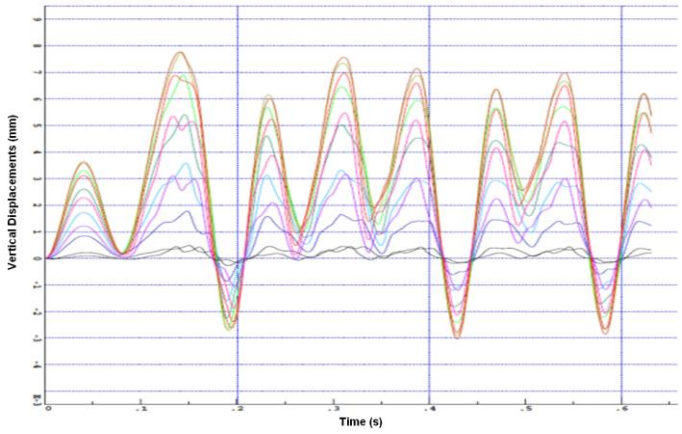


(c) At Speed of 310 km/h

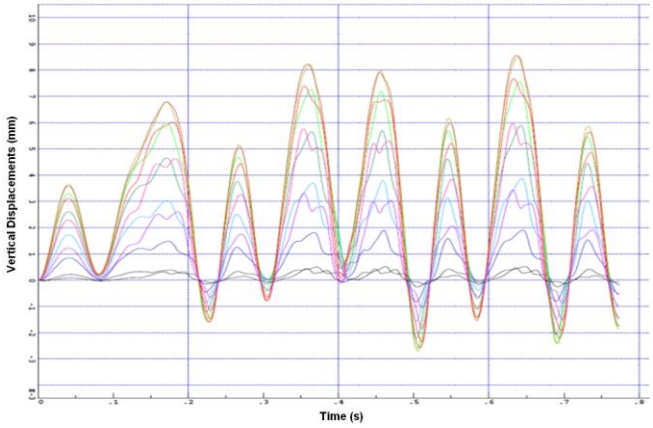


(d) At Speed of 380 km/h

Figure 5 Time Histories of Vertical Deflections of Each Bridge Beam Segments

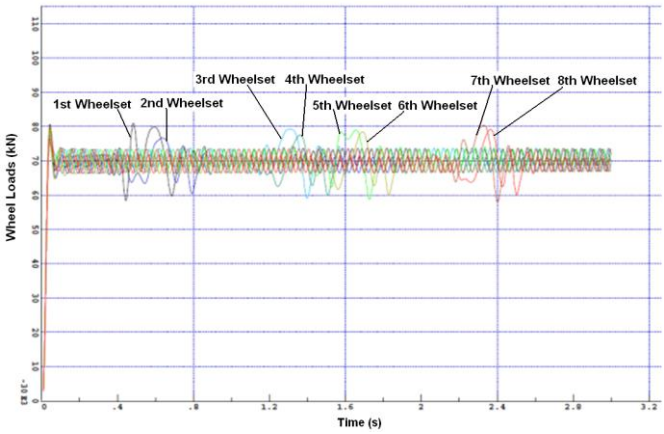


(a) At Speed of 80 km/h

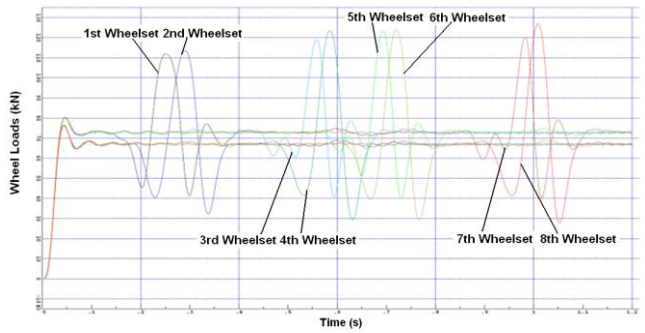


(b) At Speed of 200 km/h

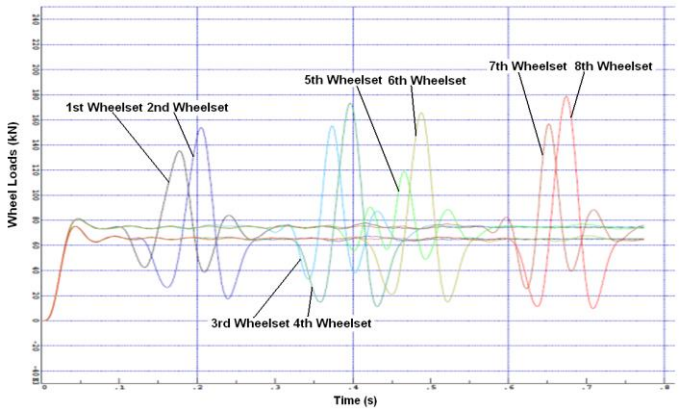


(c) At Speed of 310 km/h

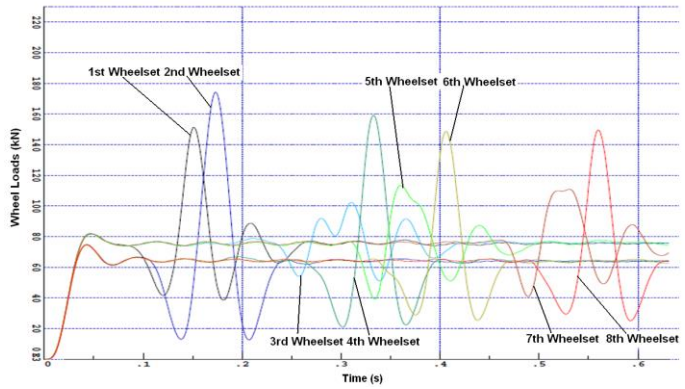


(d) At Speed of 380 km/h

Figure 6 Time Histories of Wheel Loads on Each Wheelset

In Eq. (9), the minimum distance of two effective loadings is defined. Fig. 6 clearly shows the first, second, third and fourth wheel impact loads from each passenger car due to the train moving on the bridge and due to the sudden change of beam bending stiffness and structure. The minimum distance of wheel loads seems to be the wheelbase (the distance between two adjacent wheelsets, e.g., 2.6m in the train modelling), as defined as the minimum distance of two adjacent loads [8]. However, under some circumstances, the minimum distance of two effective loadings was defined as the length of a passenger car [9] and [14]. It is thought that this distance is dependent upon the deflection responses of bridge beam.

In the time histories of the vertical deflections of each bridge beam segments shown in Fig. 5, it is clearly shown that the vertical deflection peak response is due to the combination of two adjacent wheelsets. This means that one bogie acts as a single effective loading when the train is moving on the bridge. Therefore, the minimum distance of two effective loadings can be identified as the distance between the rear bogie of a passenger car and the front bogie of the car behind it. In the train modelling, this distance is about 3.955×2 m, so, the critical train speed is $V_{cr} = d \times f_{n0} \times 3.6$ = 3.955×2×10.54×3.6 = 300 km/h.

In the bridge design practice, the impact factor ***I*** is used to account for the amplification effect of the bridge due to the passage of moving vehicles through increase of the design forces and stresses. The impact factor ***I*** to be used in this study is defined as:

$$I = \frac{R_d(x) - R_s(x)}{R_s(x)} \qquad (10)$$

where $R_d(x)$ and $R_s(x)$ denote the maximum dynamic and static responses of the bridge respectively at $x$ direction caused by the moving train. Generally, one of responses – vertical deflection is used to calculate the impact factor. The maximum static vertical deflection can be obtained using a formula –

$$\delta_{msd} = 0.5 \times W_{Car} \times \frac{L^3}{192EI} = 4.26 \times 10^{-3}\ \text{m}$$

Therefore, the impact factor based on the vertical deflection is plotted in Fig. 7.

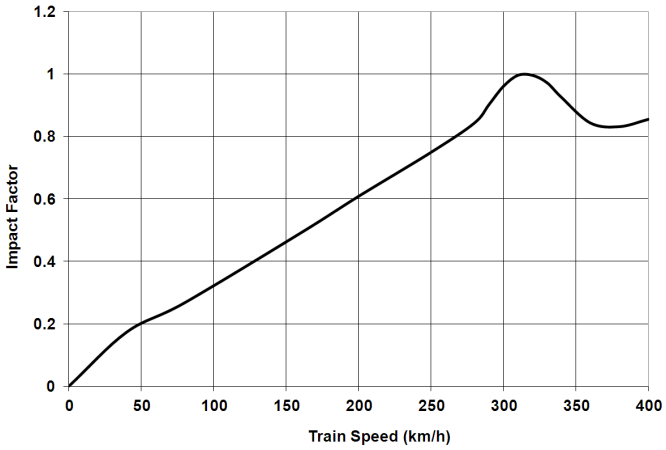


Figure 7 Impact Factor

From Fig. 7, it can be seen that the impact factor reaches the maximum value (about 1.0) at the train speed of 310 km/h, which is much closed to the simple calculation of 300 km/h. It can be also seen from Fig. 5 (c) that at the speed of 310 km/h, the wave length is about 8 m. It can be concluded that the critical train speed for this type of train and of bridge will be 310 km/h. The dynamic factor, whose definition is the same as the impact factor, but based on the dynamic wheel load, is also plotted and shown in Fig. 8 (a). The corresponding wheel unloading rate, which is defined as 1- the minimum wheel load / the static wheel load and its unit is the percentage, is plotted in Fig. 8 (b).

Comparing Fig. 8 (a) with Fig. 7, the dynamic factor is much larger than the impact factor. When the speed is at 310 km/h, the dynamic factor reaches the maximum value, about 1.56. The purpose of plotting the wheel unloading rate is to examine the vertical stability of train moving on the bridge. The Australian RISSB standard [19] requests the wheel unloading rate to be always less than 90%. Although the simulated results do not exceed the limit of 90%, it is close to the limit when the train is running at the critical speed of 310 km/h, e.g., 86.4%.

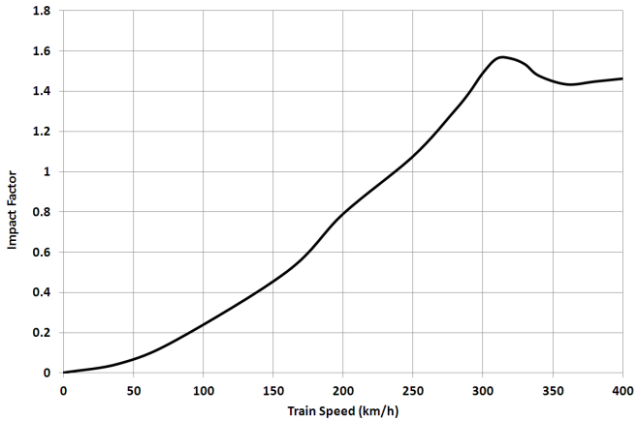


(a) Dynamic Factor

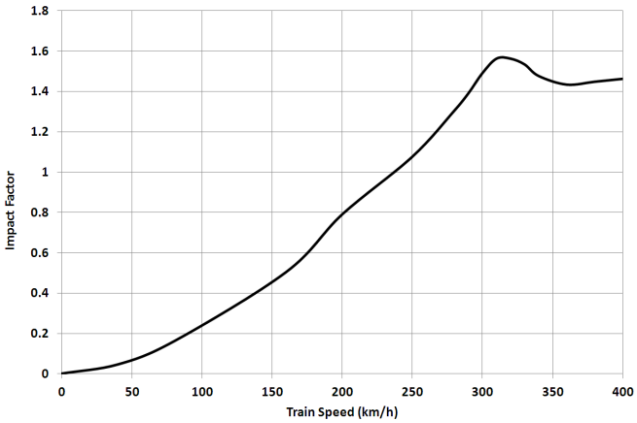


(b) Wheel Unloading Rate (%)

Figure 8 Dynamic Wheel Load versus Train Speed

### *4.2 Two-Span Bridge*

A real two-span bridge shown in Fig. 9 was considered in order to compare the measured strain gauge data [20] with the simulated ones. The bridge has two layers – reinforced concrete slabs and universal beams.

(a) Bridge, looking south.

(b) Bridge, looking north.

Figure 9 a Real Two-Span Bridge

In the report [17], the span length is the only available parameter with 3.285 m. Hence, the rail and the bridge modelling are almost the same as those in the Section 4.1 except that there is a pier supporting the bridge at the bridge middle, as shown in Fig. 4. Some of the following parameters listed in Table 2 are assumed.

Table 2 Basic Parameters for Bridge

| Young's Modulus E (GPa) | Second Moment of Area I ($m^4$) | Span Length L (m) | Weight Per Length m (kg/m) |
|---|---|---|---|
| 200* | $9.5\times10^{-4*}$ | 3.285 | 2400* |

*Assumed values based on trial simulations

If the parameters in Table 2 are substituted into Eq. (8) and Eq. (9) to calculate the train critical speed, this speed value is much higher than allowed train speed. During the field measurement, the speed of train's passing over the bridge is about 160 km/h. Fig. 10 shows the time histories of the vertical deflections of each bridge beam segments, simulated at the speed of 160 km/h using Gensys. It can be seen that when the train passes over each span, it leaves the four deflection peaks on each span due to the four bogies.

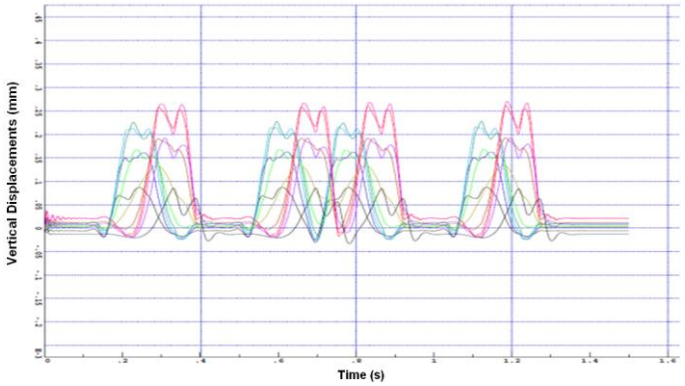


Figure 10 Time Histories of Vertical Deflections of Each Segment

The installation positions of strain gauges are close to the middle pillar about 0.5 m away. Fig. 11 (a) shows the measured beam longitudinal strain values with filtered using 20 Hz low-pass. It can be guessed from Fig. 11 (a) that the train is comprised of more than three passenger cars. Fig. 11 (b) shows the simulated vertical deflection near the measurement point. The trend of the data in these two graphs is consistent.

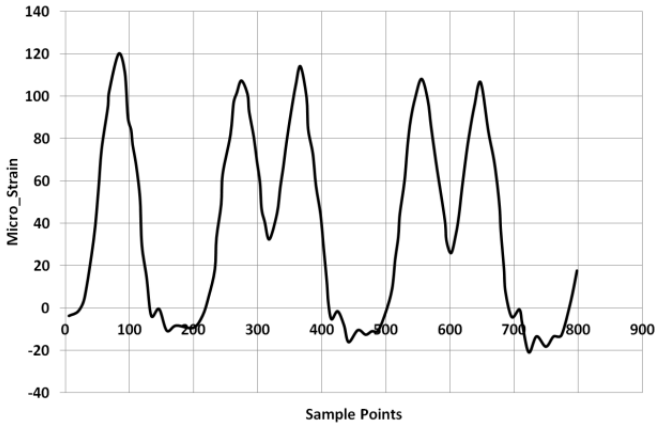


(a) Measured Strain Values

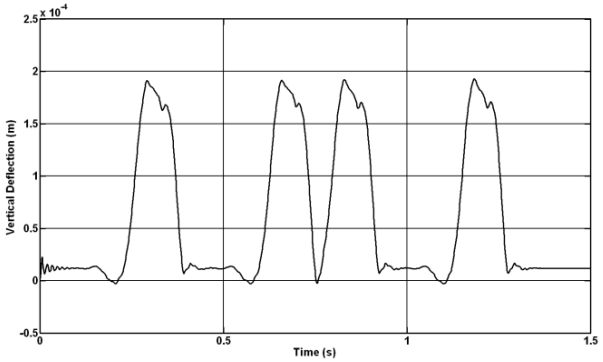


(b) Vertical Deflection near Measurement Point

Fig. 11 Change Trend Comparison

The relationship between strain and deflection in the beam may be expressed as:

$$\varepsilon_x = -z\frac{\partial^2 w}{\partial x^2} \quad (11)$$

where $z$ is the distance to the beam neutral axis. The value of $z$ is taken as 0.25m for the calculation. The centered difference formulas for the five–point stencils approximation is used to numerically solve the Eq. (11) according to the data shown in Fig. 11 (b). The solution result is shown in Fig. 12. Comparing Fig. 12 with Fig. 11 (a), the change trend is consistent and the absolute amplitude of the peak value is equivalent.

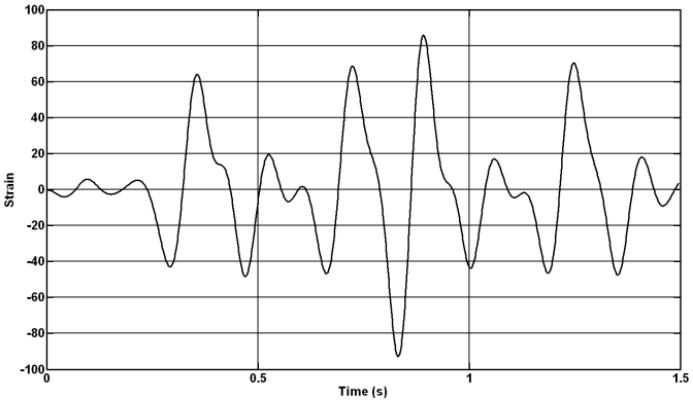


Figure 12 Numerical Solution of Eq. (11)

The simulations for the train passing the bridge at the speed of 160 km/h are graphically shown in Fig. 13.

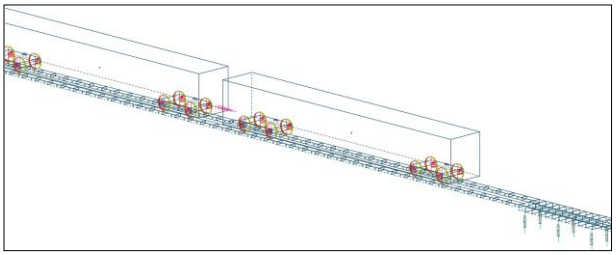

(a) Simulation Start

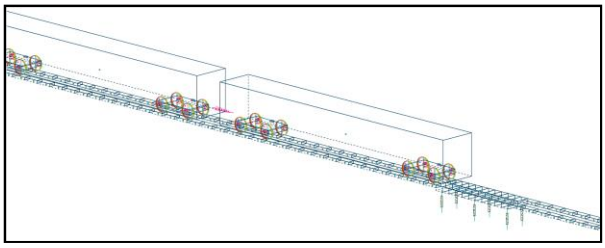

(b) Start to Pass Bridge

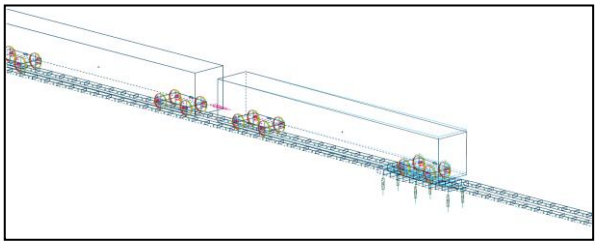

(c) First Bogie on Bridge

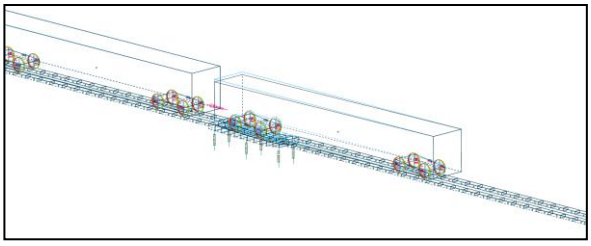

(d) Second Bogie on Bridge

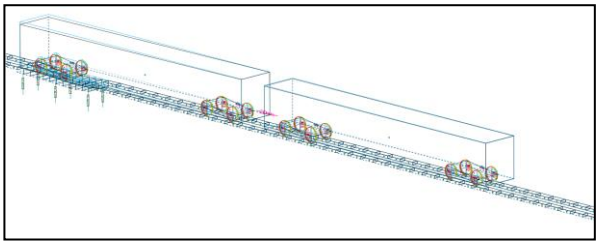

(e) Last Bogie on Bridge

(f) Train Passing over Bridge

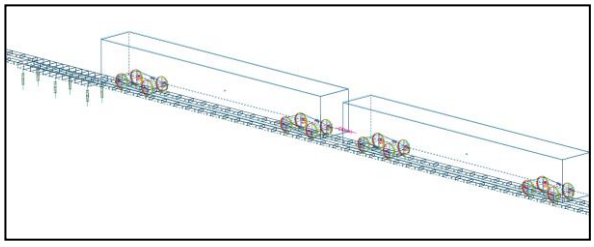

Figure 13 Train Passing Bridge in Gensys multibody software

## 5 CONCLUDING REMARKS

A rail train-track/bridge dynamic interaction model – including a comprehensive rail train model using multi-body dynamics approach and a flexible track/bridge model using Euler–Bernoulli beam theory was generated using Gensys software in order to investigate the bridge's dynamic behaviours and characteristics due to a train moving on it.

Two kinds of bridges were selected for the simulations. One is a single span bridge and the other is a two-span bridge. In the first kind of bridge, the basic parameters were so chosen so that the train critical speed can be determined within reasonable speed range. One of the important parameters to influence the critical speed is the minimum distance of two effective loadings because the critical speed increases proportionally (1:1) to the minimum distance of two effective loadings. Generally, it was defined as the minimum distance of two adjacent loads. For a single rail vehicle, it would be the wheelbase. However, in this case study, the minimum distance of two effective loadings could be identified as the distance between the rear bogie of a passenger car and the front bogie of the car behind it. However, under some circumstances, the minimum distance of two effective loadings was defined as the length of a passenger car when the rear bogie of a passenger car and the front bogie of the car behind it were made much closed to each other.

The impact factor based on the vertical deflection and the dynamic factor based on the dynamic wheel load have been plotted. In the situation of the train and bridge interaction in this paper, it is apparently shown that the dynamic factor is much larger than the impact factor. It is possible for the impact factor to be larger than the dynamic factor in other situations. It is suggested that both factors are considered in bridge design procedure and then the larger one is used for the calculations.

For the simulation of a real bridge with two spans, the simulated data is consistent with the measured values.

## Acknowledgments

The authors are grateful to the CRC for Rail Innovation (established and supported under the Australian Government's Cooperative Research Centres program) for the funding of this research. Project No. R3.118 "Life Cycle Management of Bridge". The authors also acknowledge the support of the Centre for Railway Engineering and the many industry partners that have contributed to this project, and in particular staff from Rio Tinto and V/Line Victoria.

## 6 REFERENCES

Xia, H., Zhang, N., and Roeck, G.D., "Dynamic analysis of high speed railway bridge under articulated trains." *Computers and Structures* V. 81, 2003, pp. 2467–2478.

Xia, J.H., Wei, Q.C., Jin, S., and You, L.X., "Dynamic Performance Evaluation of Bridge-Subgrade Transition of Shuohuang Railway." 2010 International Conference on Measuring Technology and Mechatronics Automation.

Nguyen, D. V., Kim, K. D., and Warnitchai, P., "Simulation procedure for vehicle–substructure dynamic interactions and wheel movements using linearised wheel–rail interfaces." *Finite Elements in Analysis and Design* V. 45, 2009, pp. 341-356.

Xia, H. Han, Y. Zhang, N. and Guo, W. "Dynamic analysis of train–bridge system subjected to non-uniform seismic excitations." *Earthquake Engng Struct. Dyn*. V. 35, 2006, pp. 1563–1579.

WU, Y. YANG, Y. and YAU, J., "Three-Dimensional Analysis of Train-Rail-Bridge Interaction Problems", *Vehicle System Dynamics*, 2001, Vol. 36, No. 1, pp. 1-35.

GYÖRGYI, J. and SZABÓ, G., "DYNAMIC TRAIN-BRIDGE INTERACTION AT AN ARC BRIDGE IN THE CASE OF A DIFFERENT MODEL." *Slovak Journal of Civil Engineering*, V. 3, No. 4, 2006, pp. 37-47.

LI, Q., XU, Y. L., WU, D. J. and CHEN, Z. W., "Computer-aided Nonlinear Vehicle-bridge Interaction Analysis." *Journal of Vibration and Control*, 00(0): 1–26, 2010. DOI: 10.1177/1077546309341603.

Yau, J. D., "RESONANCE OF CONTINUOUS BRIDGES DUE TO HIGH SPEED TRAINS." *Journal of Marine Science and Technology*, Vol. 9, No. 1, pp. 14-20, 2001.

Wang, Y. Wei, Q. Shi, J. and Long. X., "Resonance characteristics of two-span continuous beam under moving high speed trains." *Latin American Journal of Solids and Structures*, V. 7, 2010, pp. 185 – 199.

Zhang, Z. C., Lin, J. H., Zhang, Y. H. Howson W. P., and Williams, F. W., "Non-stationary random vibration analysis of three-dimensional train–bridge systems." *Vehicle System Dynamics*, Vol. 48, No. 4, April 2010, pp. 457–480.

Xin T. and Gao, L., "Reducing slab track vibration into bridge using elastic materials in high speed railway." *Journal of Sound and Vibration*, 2010, doi:10.1016/j.jsv.2010.11.023.

Chan, T. H.T., Guo, L. and Li, Z.X., "Finite element modelling for fatigue stress analysis of large suspension bridges." *Journal of Sound and Vibration* V. 261, 2003, pp. 443–464.

Song, M. K., Noh, H. C., and. Choi, C. K., "A new three-dimensional finite element analysis model of high-speed train–bridge interactions." *Engineering Structures*, V. 25 2003, pp. 1611–1626.

Kwark, J. W., Choi, E. S., Kim, Y. J. Kim, B. S., and Kim, S.I. "Dynamic behaviour of two-span continuous concrete bridges under moving high-speed train" *Computers and Structures* V. 82, 2004, pp. 463–474.

Liu, K., Reynders, E., DeRoeck, G., and Lombaert, G., "Experimental and numerical analysis of a composite bridge for high-speed trains" *Journal of Sound and Vibration*, V. 320, 2009, pp. 201–220

Imam, B. M., Righiniotis, T. D., and Chryssanthopoulos, M. K., "Numerical modelling of riveted railway bridge connections for fatigue evaluation" *Engineering Structures*, V. 29, 2007, pp. 3071–3081.

Sun, Y.Q, Cole, C. Dhanasekar, M, and Thambiriratnam, D.P, "Modelling and analysis of the crush zone of a typical Australian passenger train", *Vehicle System Dynamics*, ISSN 1744-5159 Vol. 50, No. 7, pp. 1137-1155.

Sun, Y.Q. and Simson, S., "A Nonlinear Three-dimensional Wagon-track Model for The Investigation of Rail Corrugation Initiation on Curved Track", *Vehicle System Dynamics*, Vol. 45, No. 2, pp. 113-132.

AS7509.3-AS_7509.3, "Railway Rolling Stock – Dynamic Behaviour – Part 3 – Passenger", 9 Mar 09.

Peng, D., and Elston, J., "Preliminary Report on the REPOS for V/Line Bridge 44", Rail CRC Project Report, 14th June, 2012.

## Appendix - I Basic parameters

| | | |
|---|---|---|
| **Mass** | | |
| Car Body | 39.4 | tonnes |
| Bogie Frame | 5.0 | tonnes |
| Wheelset | 1.9 | tonnes |
| **Suspension & Coupler Stiffness & Damping** | | |
| Lateral stiffness at centre bearing rim | 5e6 | N/m |
| Longitudinal stiffness at centre bearing rim | 20e6 | N/m |
| Secondary suspension stiffness (4 per bogie) | 10.7e6 | N/m |
| Secondary suspension damper (4 per bogie) | 0.2e6 | Ns/m |
| Primary suspension coil Spring (8 per bogie) (longitudinal and lateral shear, and vertical stiffness) | 24e6, 1.5e6, 0.73e6 | N/m |
| Primary suspension damping (8 per bogie) (longitudinal, lateral and vertical damping) | 2.5e3, 1.5e3, 0.3e6 | Ns/m |
| Coupler stiffness | 0.58e6 | N/m |
| **Dimensions** | | |
| Bogie wheel base | 2.6 | m |
| Bogie centres | 16.8 | m |
| Car length | 24.71 | m |